Assignment of the Nonexchanging Protons of the α-Spectrin SH3 Domain by Two- and Three-Dimensional $^1H-^{13}C$ Solid-State Magic-Angle Spinning NMR and Comparison of Solution and Solid-State Proton Chemical Shifts

Barth-Jan van Rossum,* Federica Castellani, Kristina Rehbein, Jutta Pauli, and Hartmut Oschkinat*[a]

The assignment of nonexchanging protons of a small microcrystalline protein, the α-spectrin SH3 domain (7.2 kDa, 62 residues), was achieved by means of three-dimensional (3D) heteronuclear ($^1H-^{13}C-^{13}C$) magic-angle spinning (MAS) NMR dipolar correlation spectroscopy. With the favorable combination of a high B_0-field, a moderately high spinning frequency, and frequency-switched Lee-Goldburg irradiation applied during ^1H evolution, a proton linewidth ≤ 0.5 ppm at 17.6 Tesla was achieved for the particular protein preparation used. A comparison of the solid-state ^1H chemical shifts with the shifts found in solution shows a remarkable similarity, which reflects the identical protein structures in solution and in the solid. Significant differences between the MAS solid- and liquid-state ^1H chemical shifts are only observed for residues that are located at the surface of the protein and that exhibit contacts between different SH3 molecules. In two cases, aromatic residues of neighboring SH3 molecules induce pronounced upfield ring-current shifts for protons in the contact area.

KEYWORDS:

NMR spectroscopy · protein structures · SH3 domains · structure elucidation

Introduction

Magic-angle spinning nuclear magnetic resonance (MAS NMR) dipolar correlation spectroscopy is rapidly developing into a technique for de novo structure determination of biological systems.[1] While dipolar correlation spectroscopy focusing on ^{13}C or ^{15}N nuclei is now being used routinely in assignment and structure refinement studies of multiply isotope enriched organic or biological solids,[1–8] ^1H MAS NMR has not yet found a similarly widespread application. This is due to the combined effect of the strong homonuclear dipolar interactions between the abundant protons in the solid state and the small proton chemical shift dispersion, which limits the resolution in the ^1H spectrum.

On the other hand, the high abundance and gyromagnetic ratio γ of the protons offers at the same time an attractive potential for correlation spectroscopy in structural research. For example, $^1H-^{13}C$ dipolar interactions are about four times stronger than the homonuclear ^{13}C dipolar couplings and, hence, heteronuclear correlations are readily obtained. Furthermore, polarization exchange mediated through the strong ^1H homonuclear interactions is easy to establish.[9–11] This will be important for the collection of structural restraints, since protons are located at the exterior of the carbon skeleton and interresidue distances d_{CH} and d_{HH} are generally shorter than the d_{CC}. Hence, both the high γ value and the advantageous spin topology favors the use of protons in intermolecular or interresidual polarization transfer. Along these lines, several examples of the application of two-dimensional (2D) $^1H-^{13}C$ heteronuclear correlation spectroscopy and 2D ^1H homonuclear single- and double-quantum spectroscopy to study hydrogen bonding and to obtain CH and HH distance information have been reported recently.[12–15]

A prerequisite for the integration of protons in structure determination concepts is sufficient resolution of the ^1H spectrum to enable an unambiguous assignment and for separating the various interactions under consideration. The most straightforward way to obtain improved proton resolution is by exploiting the large chemical shift dispersion of a second type of nucleus (for example, ^{13}C or ^{15}N) or of the heteronuclear dipolar couplings (such as $^1H-^{13}C$ or $^1H-^{15}N$) in multidimensional correlation spectroscopy.

Of equal importance is the fact that the homogeneous broadening arising from the $^1H-^1H$ couplings can be partly

[a] *Dr. B.-J. van Rossum, Prof. H. Oschkinat, F. Castellani, K. Rehbein, Dr. J. Pauli*
Forschungsinstitut für Molekulare Pharmakologie
Robert-Rössle-Strasse 10, 13125 Berlin (Germany)
Fax: (+49) 30-94793-169
E-mail: brossum@fmp-berlin.de, oschkinat@fmp-berlin.de

  1439-4227/01/02/12 $ 17.50+.50/0 CHEMBIOCHEM **2001**, 2, 906 – 914

removed by application of radio frequency (RF) schemes that manipulate the spin Hamiltonian and effectively decouple the proton spins. Techniques based on Lee-Goldburg (LG) irradiation[16] have proven particularly useful for this aim, since they can be combined with elevated MAS frequencies. Frequency-switched LG (FSLG) or phase-modulated LG (PMLG) irradiation applied during indirect ^{1}H detection significantly enhances the proton resolution.[17–19] Alternatively, during ^{1}H observation, the semi-windowless WHH-4 sequence can be applied successfully.[20] Finally, a high magnetic field induces a line-narrowing effect on the proton response,[12, 21, 22] which, in combination with an increased chemical shift dispersion, will help to increase the resolution.

The application of solid-state NMR technology to obtain structural information of progressively larger biological systems was initiated many years ago, but is not yet fully established. In this paper, we focus on the assignment of the ^{1}H signals of a microscopically ordered, moderately sized, and uniformly ^{13}C,^{15}N-enriched protein in the solid state and on the linewidth that is achievable. We show that it is possible to arrive at an almost complete solid-state NMR assignment of the nonexchangeable proton responses of the α-spectrin SH3 domain (7.2 kDa, 62 residues). The assignment was achieved by means of high-field FSLG-decoupled 2D (^{1}H – ^{13}C) and 3D (^{1}H – ^{13}C – ^{13}C) heteronuclear dipolar correlation spectroscopy, based on the ^{13}C and ^{15}N assignment published earlier.[8, 23] The comparison of the solution- and solid-state chemical shifts suggests identical structures in both states, and similar crystal packing in our solid preparation and the one from which the crystal structure was derived.

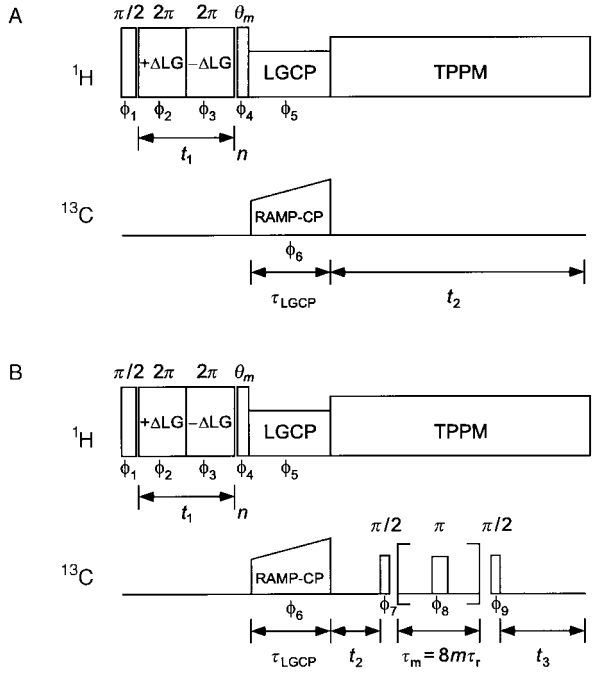

Figure 1. *Pulse programs used for the 2D (A) and 3D (B) heteronuclear dipolar correlation experiments. During proton evolution in t_1, FSLG decoupling is applied. The phase listing in (A) is according to ϕ1 = x, −x,y, −y, −x,x, −y,y; ϕ2 = x,x,y,y, −x, −x, −y, −y; ϕ3 = −x, −x, −y, −y,x,x,y,y; ϕ4 = −y, −y,x,x,y,y, −x, −x; ϕ5 = y,y, −x, −x, −y, −y,x,x, −y −y,x,x,y,y, −x, −x; ϕ6 = x,x, −x, −x,y,y, −y, −y and ϕadc = x, −x, −x,x,y, −y, −y,y, −x,x,x, −x, −y,y,y, −y. The phase listing in (B) is ϕ1 = x, −x, −x,x; ϕ2 = x,x, −x, −x; ϕ3 = −x, −x,x,x; ϕ4 = −y, −y,y,y; ϕ5 = y,y, −y, −y, −y,y,y; ϕ6 = x,x, −x, −x,y,y, −y; ϕ7 = y,y, −y, −y,x,x, −x, −x, −y, −y,y,y, −x, −x,x,x; ϕ8 = y, −x,y, −x, −x,y, −x,y; ϕ9 = x,x, −x, −x,y,y, −y, −y and ϕadc = y, −y, −y,y, −x,x,x, −x, −y,y,y, −y,x, −x, −x,x. TPPM = two-pulse phase modulation, RAMP-CP = ramped cross-polarization.*

Results

Recently, it was demonstrated that precipitates of the α-spectrin SH3 domain can be prepared reproducibly with a high degree of microscopical order and structural homogeneity, which lead to well-resolved MAS NMR spectra.[8, 23] From these preparations it was possible to obtain nearly complete sequence-specific assignments of the observable ^{13}C and ^{15}N signals through experiments with selective $N_iC_i^{\alpha}$ and N_iCO_{i-1} heteronuclear polarization transfer followed by a ^{13}C homonuclear correlation unit.[8] Based on this assignment of the ^{13}C resonances, the ^{1}H signals of the side chains can be assigned by multidimensional heteronuclear ^{1}H – ^{13}C dipolar correlation spectroscopy. For this purpose, we have applied a 2D LG experiment (Figure 1 A) and a 3D ^{1}H – ^{13}C – ^{13}C correlation technique (Figure 1 B).

Figure 2 shows 2D ^{1}H – ^{13}C heteronuclear dipolar correlation spectra of the α-spectrin SH3 domain recorded with the pulse program depicted in Figure 1 A, with LG cross-polarization (LGCP) mixing times τ_{LGCP} of 350 μs (Figures 2 A and B), and 2.0 ms (Figures 2 C and D). At short LGCP mixing times, a proton exchanges magnetization with its directly bonded carbon, while polarization transfer to remote carbons is relatively inefficient in a uniformly ^{13}C-labeled environment and requires longer mixing times.[13] This can be explained in terms of a truncation of the weak CH dipolar couplings to distant carbons by the strong heteronuclear dipolar interaction within the directly bonded CH spin-pair. A similar argument was recently used to account for ^{1}H – ^{15}N heteronuclear transfer processes observed in the PISEMA experiment.[24] Hence, the correlations in Figures 2 A and B mainly reflect polarization exchange between directly coupled protons and carbons. In contrast, Figures 2 C and D show a heteronuclear dipolar correlation experiment that was obtained with a relatively long τ_{LGCP} of 2.0 ms. In this dataset, correlations occur with both directly bonded and remote protons which may be intra- or interresidue ones.

From the data in Figure 2 B, a few aliphatic protons can be readily assigned through correlations with ^{13}C that show unique carbon shifts. Among these are for example the H^{β} of A55, correlated with the C^{β} at $\delta = 15.9$,[8] the H^{δ} of I30, correlated with the C^{δ} at $\delta = 11.4$, and the H^{β} of the threonines. Evidently, most of the remaining ^{1}H resonances can not be assigned unambiguously from the 2D data due to overlap in the ^{1}H and ^{13}C dimensions.

In order to increase resolution, a 3D ^{1}H – ^{13}C – ^{13}C heteronuclear dipolar correlation experiment of the α-spectrin SH3 domain was recorded with the pulse program depicted in Figure 1 B. The 3D experiment embodies a straightforward combination of the 2D ^{1}H – ^{13}C FSLG-decoupled heteronuclear correlation experiment in Figure 1 A with the radio frequency

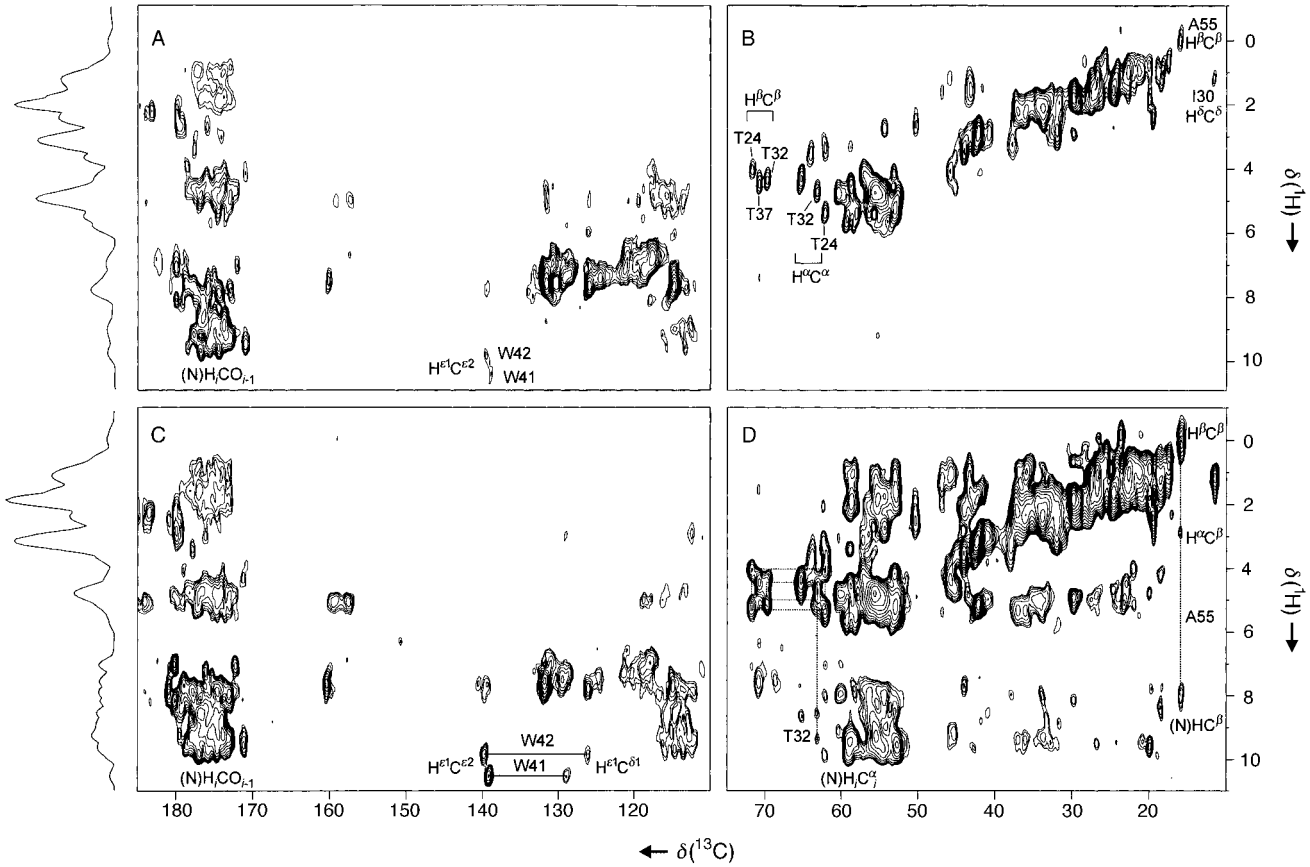

Figure 2. *Contour plots and ^{1}H projections of two 2D FSLG-decoupled ^{1}H – ^{13}C heteronuclear dipolar correlation spectra of a microcrystalline [U-^{13}C, ^{15}N] α-spectrin SH3 domain sample, recorded at a field of 17.6 T and a spinning frequency of $\omega R/2\pi = 11.5$ kHz. The data were obtained with an LGCP contact of 350 μs (A, B) or 2.0 ms (C, D).*

driven dipolar recoupling (RFDR) technique, which recouples in the second transfer step the ^{13}C homonuclear dipolar interactions that are otherwise averaged by sample spinning.[2, 25] To maintain selectivity during the heteronuclear transfer, a short τ_{LGCP} of 350 μs was applied in the 3D experiment.

The assignment procedure applied to the 3D dataset is illustrated in Figure 3. Figure 3 A shows a contour plot of a 2D ^{13}C homonuclear RFDR spectrum of the α-spectrin SH3 domain. The lines in the figure specify the correlation network of a selected residue, V58. Figure 3 B shows several ^{1}H – ^{13}C ($\omega1 - \omega3$) slices extracted from the 3D experiment. The numbering of the slices corresponds with the numbering of the correlations in Figure 3 A and helps to keep track of the $\omega2$ positions of the respective signals in the 3D spectrum. For instance, the numbers 1 and 2 in Figure 3 A mark the valine residue's correlations of the C$^{\gamma2}$ at $\delta =$ 19.6 ($\omega2$) with the C$^{\alpha}$ and C$^{\beta}$, respectively. Slice 1 shows the corresponding H$^{\gamma2}$ – C$^{\gamma2}$ – C$^{\alpha}$ cross-peak in the 3D spectrum with a ^{13}C$^{\alpha}$ ($\omega3$) shift around $\delta = 57.9$, while slice 2 represents the H$^{\gamma2}$ – C$^{\gamma2}$ – C$^{\beta}$ correlation with a $\omega3$ shift of $\delta = 35.6$ for the C$^{\beta}$. From these slices it is possible to assign the H$^{\gamma2}$ of V58 unambiguously. In a similar way, slices 3 – 6 provide the chemical shifts of the H$^{\beta}$ and H$^{\alpha}$ for the selected valine.

This procedure can be extended to assign other protons, and we were able to arrive at an almost complete assignment of the observable proton signals. The solid-state shifts δ_{solid} are listed in Table 1. Some of the residues are not included in the table, since for these residues no solid-state NMR signal was detected with the pulse sequences employed. Among these are residues 1 – 5 at the N terminus and D62 at the C terminus. This has been reported previously and was explained in terms of the presence of multiple conformers interconverting at unfavorable rates or an interference of the increased mobility with the NMR conditions.[8, 23] Work is currently in progress to study the underlying mechanisms that lead to the apparent signal loss.

The solid-state proton assignment obtained from the 3D spectrum requires the carbon assignment as input. On the other hand, due to the additional proton dimension the overall resolution is enhanced. As a result, carbon – carbon correlations that were otherwise overlapping are now separated. An example of this improved resolution can be found in Figure 3. The correlation C$^{\alpha}$ – C$^{\gamma1}$ of V58 (tagged as "5") overlaps with the C$^{\alpha}$ – C$^{\gamma1}$ cross-peak of V53 in the ^{13}C – ^{13}C experiment. This overlap is resolved in the proton dimension of the 3D experiment (see slice 5 in Figure 3 B).

Discussion

In this paper we report a nearly complete proton assignment of a moderately sized protein in the solid-state, through the use of 3D heteronuclear correlation spectroscopy. The assignment was possible because of comparably narrow proton lines that are resolved in the solid-state 3D data as a result of a combination of

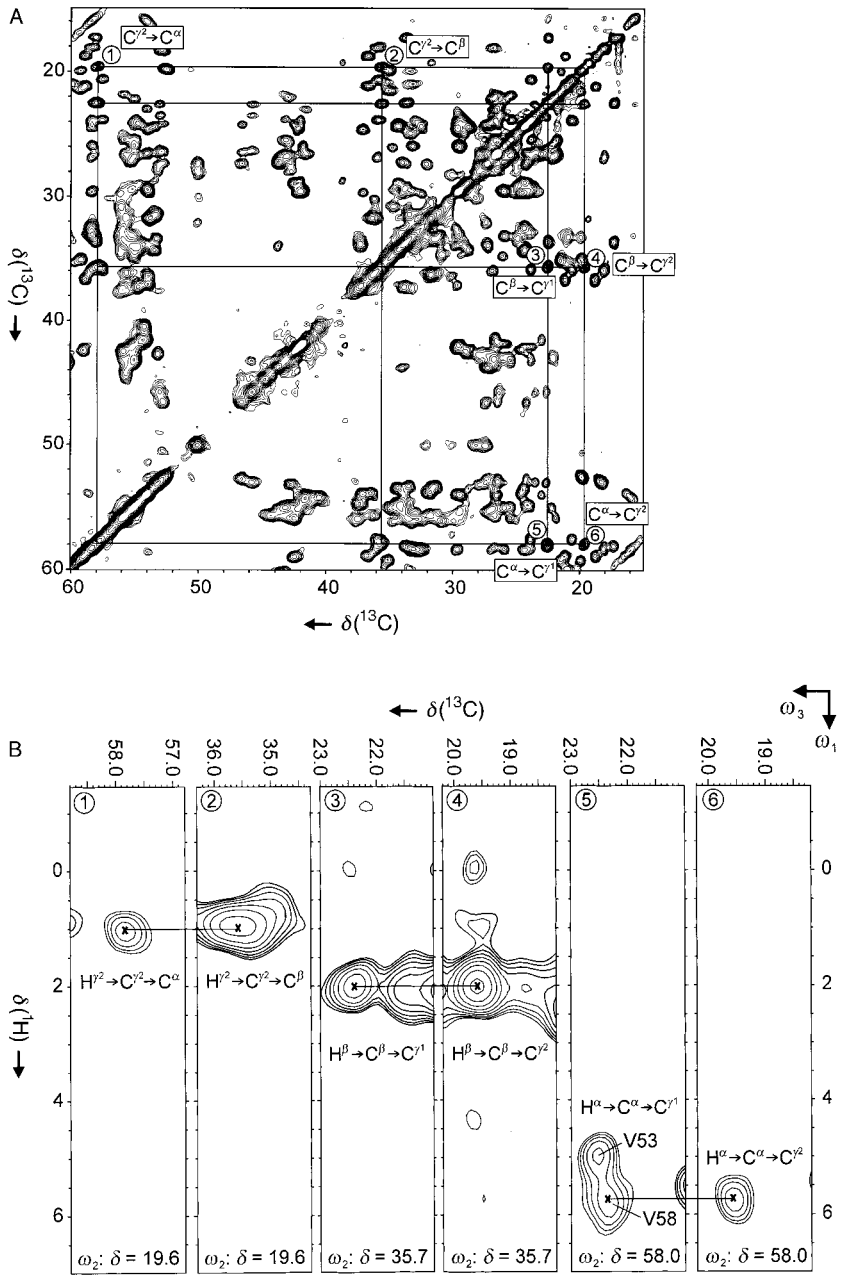

Figure 3. *Contour plot of a 2D ^{13}C homonuclear RFDR spectrum (A) and $^{1}H-^{13}C$ (ω1 – ω3) slices (B) extracted from a 3D heteronuclear ($^{1}H-^{13}C-^{13}C$) dipolar correlation spectrum of microcrystalline [U-^{13}C, ^{15}N] α-spectrin SH3 domain sample. The spectra were recorded at a field of 17.6 T and a spinning frequency of $\omega R/2\pi = 8.0$ kHz. The 3D experiment was obtained by exploiting an LGCP contact of 350 μs and RFDR mixing of 2.0 ms. The numbering of the correlations in (A) corresponds with the numbering of the slices in (B).*

effective proton homonuclear decoupling, which reduces the homogeneous line width, and the high degree of structural order in our sample that minimizes the inhomogeneous line broadening.

The short LGCP contact time of 350 μs applied in the 3D experiment for the transfer of polarization from ^{1}H to ^{13}C results in highly selective correlations between directly bonded CH pairs, due to heteronuclear dipolar truncation effects in the uniformly ^{13}C enriched preparation. On the other hand, protons that are not bound to a ^{13}C atom, for instance protons attached to a nitrogen atom, can transfer polarization within a short LGCP contact to adjacent nonprotonated carbons.[13] In such spin clusters only weak heteronuclear couplings are present, and the truncation picture sketched above clearly does not hold. An example of this effect is illustrated in Figure 2 A, where correlations between the $NH^{\varepsilon 1}$ protons of the tryptophan side chains and the neighboring quarternary $C^{\varepsilon 2}$ are observed, while correlations involving the equally distant but protonated $C^{\delta 1}$ are of much lower intensity. A more interesting manifestation of the same effect is found in the range $\delta = 7-10$ and involves NH proton responses correlating with the CO_{i-1} of the preceding amino acid, that resonate with a ^{13}C chemical shift around $\delta = 175$ (Figure 2 A). In contrast, polarization transfer from the NH_i to the C_i^{α} during the short τ_{LGCP} of 350 μs is less efficient due to the presence of the strongly coupled H_i^{α} (Figure 2 B).

In the 2D $^{1}H-^{13}C$ heteronuclear correlation spectrum recorded with a long contact time of 2.0 ms, protonated carbons receive additional polarization from remote protons (Figures 2 C and D). Although the spectrum is not selective in the sense that each ^{13}C atom receives only polarization from its directly bonded proton, the transfer events are still well-defined. For instance, the C^{β} of the alanines correlate with their own H^{β} and H^{α} and with a backbone amide proton, but not with ^{1}H from other side chains. Likewise, for the threonine networks, transfer processes of the form $H^{\alpha} \rightarrow C^{\beta}$, $H^{\gamma} \rightarrow C^{\beta}$, and $H^{\beta} \rightarrow C^{\alpha}$ are observed. At this long mixing time, correlations of the C^{α} with more than one backbone amide protons are now detected. Particularly resolved are the correlations involving the C^{α} of T32, that resonates around $\delta = 62.9$, well-separated from most other C^{α} signals. The C^{α} of this threonine shows correlations with two resolved NH protons, that we tentatively assign to its own and that of the neighboring amino acid L33.[26] Such sequential polarization transfer events may assist the sequential assignment, but prevents the assignment of the NH resonances with the present data set. Work to assign the NH protons, and to study transfer processes involving these protons in detail is currently in progress.

Once the solid-state proton assignment has been obtained, it is instructive to compare the chemical shifts of the protons in the solid state δ_{solid} with the shifts δ_{liquid} obtained by solution NMR. The solution data have been recorded at two different pH values, pH 3.5 and pH 7.3. The pH 7.3 data are closest to those of our

Table 1. *^{1}H solid-state chemical shifts and ^{1}H solution chemical shifts (in italics; measured at pH 7.3 and T = 300 K) of the α-spectrin SH3 domain.*[a]

Residue	Chemical shift (δ)[b]									
	H^{α}	H^{β}	H^{γ}	$H^{\gamma1}$	$H^{\gamma2}$	H^{δ}	$H^{\delta1}$	$H^{\delta2}$	H^{ε}	H^{ζ}
E7	4.8	2.1	1.8							
	4.46	*1.96*	*2.25/2.20*							
L8	5.3	1.0	0.9				− 0.5	[0.7][c]		
	5.39	*1.74/1.34*	*1.70*				*0.81*	*0.78*		
V9	5.3	1.9		1.0	0.8					
	5.16	*1.99*		*1.04*	*0.78*					
L10	5.2	1.4	1.0				0.8	0.9		
	5.12	*1.69/1.36*	*1.27*				*0.80*	*0.82*		
A11	4.6	1.6								
	4.59	*1.66*								
L12	4.1	1.3/0.5	1.5				0.7	0.7		
	3.88	*1.17/0.7*					*0.68*	*0.62*		
Y13	4.5	3.2/1.6								
	4.58	*3.05/2.08*								
D14	4.7	2.7								
	4.61	*2.82/2.57*								
Y15	4.7	3.0								
	4.64	*3.00/2.89*								
Q16	4.6	1.8	2.3							
	4.45	*1.78*	*2.27*							
E17	4.3	1.8	1.8							
	4.23	*2.16/1.83*	*2.16*							
K18	4.6	1.8	1.4			1.5(0.3)[d]			2.9	
	4.43	*2.00*	*1.67/1.48*			*1.73*			*3.08*	
S19	4.3	3.3/4.0								
	4.86	*3.73/4.09*								
P20	4.6	2.3/1.7	2.0			2.3				
	4.56	*2.47/1.95*	*2.07/1.98*			*3.88/3.77*				
E22	5.3	[2.3]/1.9	2.2							
	5.45	*2.75/2.18*	*2.35/2.05*							
V23	4.6	1.9		0.7	0.6					
	4.50	*1.82*			*0.59*					
T24	5.3	4.0	1.4							
	5.09	*3.93*	*1.34*							
M25	5.0	1.9	2.8							
	4.92	*2.22/1.83*	*2.68/2.57*							
K26	5.0	1.7	1.5			1.7			3.1	
	4.88	*1.71*	*1.41*						*3.02*	
K27	3.3	1.5	1.1			1.9			3.0	
	3.26	*1.58/1.52*	*1.11*			*1.59*			*2.90*	
G28	4.5/3.5									
	4.43/3.49									
D29	4.7	2.7								
	4.49	*2.81/2.49*								
I30	5.1	2.3		1.5	0.7	1.0				
	5.02	*1.77*		*1.72/1.15*	*0.91*	*0.88*				
L31	5.1	1.5	1.6				1.4(0.3)	[0.9]		
	4.99	*1.45/1.58*					*0.87*			
T32	4.7	4.3	1.3							
	4.56	*4.10*	*1.13*							
L33	4.6	1.7/1.0	1.2(0.2)				0.3	0.8		
	4.36	*1.79/1.11*	*1.14*				*0.40*	*0.68*		
L34	4.7	1.1	1.3(0.2)					0.7		
	4.51	*1.41/1.12*						*0.69*		
N35	4.8	2.8(0.3)								
	4.70	*2.73/2.68*								
S36	4.2	3.1/2.3								
	3.86	*2.82/2.02*								
T37	4.2	4.3	1.4							
	3.96	*4.21*	*1.31*							
N38	4.8	[3.9]/2.9								
	4.85	*3.70/2.90*								
D40	4.6	2.4								
	4.54	*2.62/2.25*								
W41	5.0	2.7								
	5.08	*2.93/2.81*								

Table 1. *(Continued)*

Residue	Chemical shift (δ)[b]									
	H^{α}	H^{β}	H^{γ}	$H^{\gamma1}$	$H^{\gamma2}$	H^{δ}	$H^{\delta1}$	$H^{\delta2}$	H^{ε}	H^{ζ}
W42	5.7	3.0/2.7								
	5.49	*2.94/2.80*								
K43	4.4	1.2	1.0			1.5			2.7	
	4.36	*1.52/1.17*	*0.99*			*1.30*			*2.56*	
V44	5.4	2.0		0.7	0.8					
	5.37	*2.11*		*0.79*	*0.75*					
E45	5.3	2.1	2.1							
	5.39	*1.88*	*2.05*							
V46	5.0	2.2		0.6	1.2					
	4.50	*2.11*		*0.98*	*1.03*					
D48	4.9	2.6(0.2)								
	4.33	*2.85*								
R49	4.6	2.1	1.9(0.2)			3.4				
	4.65	*1.85*	*1.77/1.59*			*3.34/3.27*				
Q50	5.9	1.8	[2.3]							
	5.52	*1.91/1.59*	*2.38/2.16*							
G51	4.0									
	3.94									
F52	5.6	3.2/2.6				7.4			7.3	7.0
	5.63	*3.17/2.60*								
V53	4.8	1.7		1.0	0.6					
					0.68					
P54	3.5	0.8/0.3	0.5			2.2				
	3.54	*1.27/0.81*	*0.65*			*2.45/2.15*				
A55	2.6	−0.2								
	2.65	*−0.06*								
A56	4.1	1.2								
	3.99	*1.18*								
V58	5.6	1.9		0.7	0.8					
	5.49	*1.89*		*0.73*	*0.74*					
K59	5.0	1.8	1.5			1.6			3.0	
	4.82	*1.73*	*1.43*			*1.70*				
K60	4.5	1.9	1.7			[2.0]			2.7	
	4.50	*2.02/1.80*	*1.66/1.44*			*1.69*				
L61	4.8	1.4	1.6				[0.5]			
	4.40	*1.60*					*0.89*	*0.87*		
	$H^{\delta1}$	$H^{\varepsilon1}$	$H^{\varepsilon3}$	$H^{\eta1}$	$H^{\zeta2}$	$H^{\zeta3}$				
W41	7.2	10.3	6.9	7.2	7.4	6.5				
W42	7.6	9.6	6.9	7.2	7.7	6.6				
		9.3								

[a] The solid-state data were calibrated by setting the shift of A55 H^{β} to $\delta = -0.24$ (see Materials and Methods). The solution shifts were obtained as described under Materials and Methods. [b] The overall error for the solid-state proton chemical shifts δ is estimated at 0.1. [c] Values within square brackets could not be assigned unambiguously. [d] Values within parenthesis indicate errors in δ larger than 0.1.

wet-solid SH3 preparation, which is prepared by precipitation from solution after increasing the pH value to ≈7.5.[23] However, the SH3 concentration at pH 7.3 is low (< 0.15 mM), and we were unable to arrive at a complete ^{1}H assignment at this pH value. For this reason, additional solution data were recorded at pH 3.5, and led to a full ^{1}H assignment. A convenient way to compare the data graphically is shown in Figure 4, where the δ_{solid} are correlated with the corresponding δ_{liquid}. All protons compared in this figure are nonexchangeable, the only exceptions being the two tryptophan NH side chain protons. In the correlation plots, the main part of the proton resonances from the two assignments is found along a straight line with relatively little scatter. A linear least-squares fit of this main response yields $\delta_{solid} = (1.003\,\delta_{liquid} + 0.18)$ for pH 3.5. The small deviation from unity in the slope can be attributed to a minor uncertainty in the determination of the LG scaling factor (see Materials and Methods). The associated error is insignificant and well within the experimental error of δ of 0.1. The offset of δ_{solid} of 0.18 suggests a small difference of the shift in the solid state and in solution of the H^{β} of A55, which was used for the calibration of the solid-state proton response. In order to avoid a systematic error in the solid-state ^{1}H shifts reported in this paper, the δ_{solid} listed in Table 1 have been recalibrated (see Materials and Methods).

The structures of the SH3 domain in the liquid[27] and solid state[28] are highly similar. This is also reflected by the overall close correspondence of the proton chemical shifts of the two states (see Figure 4 and Table 1). On the other hand, a few residues exhibit ^{1}H shifts in the solid state that are notably different from those in solution at both pH values. These

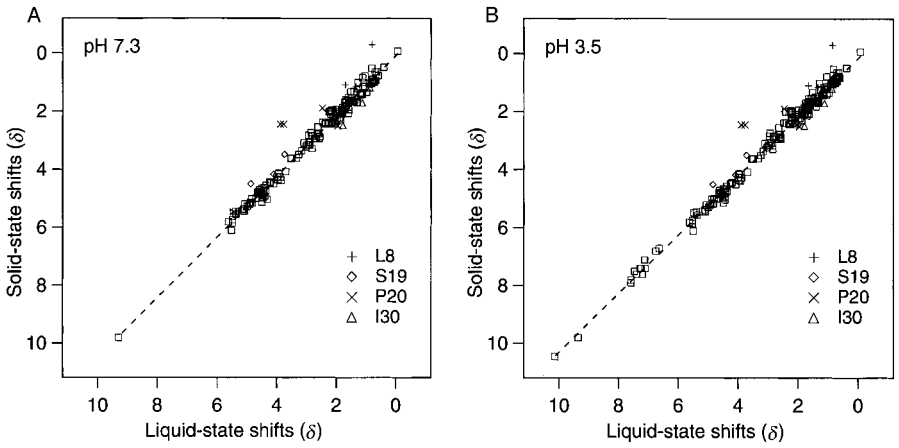

Figure 4. *Correlation plot of the solid-state proton chemical shifts versus the liquid-state shifts at pH 7.3 (A) and pH 3.5 (B). The main response (□) is found along a straight line with relatively little scatter. The dashed lines represent linear least-squares fits of the main response. Some residues (L8, S19, P20, and I30) exhibit solid-state proton shifts that differ significantly from the shifts found in solution; these are indicated in the figure.*

residues are indicated in the correlation plots (Figure 4) and their side chains are shown in a structural model of the SH3 domain in Figure 5 A. They are all located on the surface of the protein. The most significant differences between the solid- and liquid-state chemical shifts are found for the CH_2^{δ} of P20 and the $CH_3^{\delta 1}$ methyl of L8 ($\times$ and $+$ in Figure 4, respectively). The chemical shift of P20 C^{δ} is shifted upfield relative to the shifts found in solution, by -1.1 (pH 3.5) and -1.2 (pH 7.3), and the chemical shift of H^{δ}, by -1.5 for both pH values. In the structural model obtained by X-ray diffraction,[28] this proline is located above the aromatic ring of Y13 from a neighboring SH3 domain, with the C^{δ} at a distance of approximately 3.5 Å above the tyrosine ring and the two δ protons at about 3 Å (Figure 5 B). Based on computations of ring-current shifts for conjugated ring systems, upfield shifts of approximately -1.0 and -1.5 are estimated for the C^{δ} and H^{δ} in this configuration, respectively.[29] This is well in agreement with the solid-state data. Likewise, the pronounced upfield shifts detected for L8, of -1.3 at both pH values for the chemical shift of $H^{\delta 1}$, and of -1.9 (pH 3.5) or -2.2 (pH 7.3) for the $C^{\delta 1}$ relative to the liquid state, reflects the presence of the nearby phenyl ring of F52 from a second SH3 molecule in the X-ray crystal structure (Figure 5 C). These data suggest a similar crystal packing in our preparation and those used for deriving the X-ray crystal structure.

In summary, we achieved a nearly complete assignment of the observable aliphatic proton signals of a nonoriented, moderately sized (7.2 kDa) protein in the solid state. The relatively narrow lines in the proton dimension due to the FSLG decoupling and the resolution enhancement resulting from the additional ^{13}C dimensions in the 3D experiment raise the expectation that the solid-state ^{1}H responses may be of particular interest for the study of uniformly labeled ligands of membrane-integrated receptors. Although the SH3 domain provides a favorable case in terms of structural homogeneity and, hence, linewidth, we envisage that the solid-state NMR proton response of small ligands functionally bound to a receptor in a structurally unique binding pocket can be assessed. The strategy followed here can provide structural information on the basis of the chemical shift assignment. The sensitivity of protons to local structural changes within the protein environment makes them extremely suitable for probing the folding of the ligand in the receptor-bound state, by comparing the solid-state shifts to the data in solution. In addition, the positioning of protons at the outside of the molecule makes them responsive to noncovalent interactions, monitored, for example, through ring-current shifts induced by aromatic rings in the intermolecular contact area. This may offer another interesting potential in the study of the binding of receptor–ligand complexes.

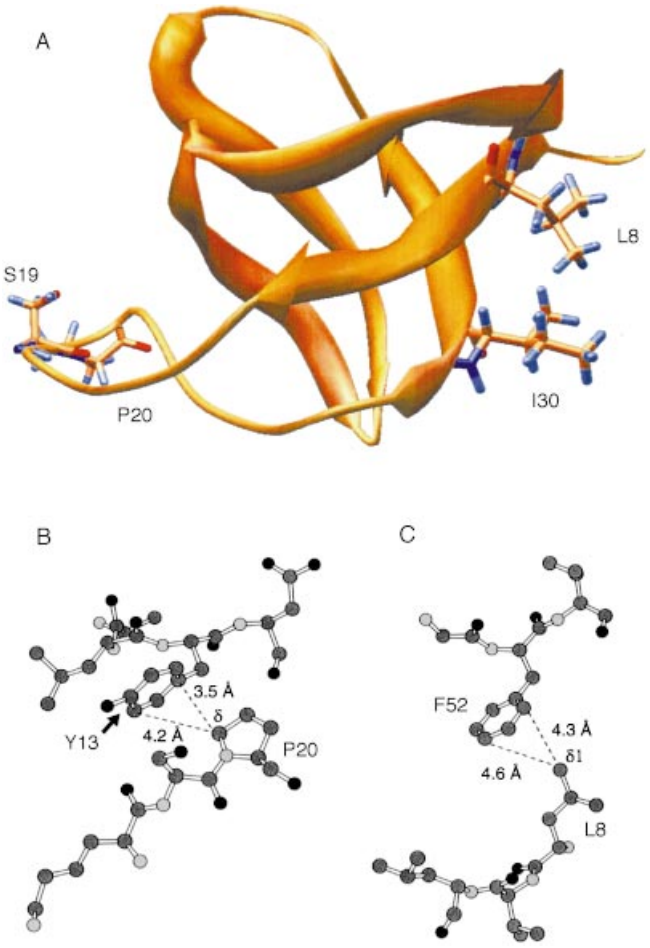

Figure 5. *A) 3D structural model of the backbone of the α-spectrin SH3 domain, according to solution NMR spectroscopy.[27] The residues that have different chemical shifts in the solid and liquid state are indicated in the figure. B) and C) Intermolecular contacts between different SH3 domains according to the crystal structure, showing in detail the contacts P20/Y13 (B) and L8/F52 (C).[28]*

Materials and Methods

All solid-state CP/MAS NMR spectra were recorded at a field of 17.6 T on a DMX-750 spectrometer, equipped with a 4 mm double-resonance CP/MAS probe (Bruker, Karlsruhe, Germany). For the correlation experiments, a preparation containing uniformly ^{13}C- and ^{15}N-enriched α-spectrin SH3 domain ($\approx$1.4 μmol; 10 mg) was used.[8] The sample was confined to the center of the rotor by use of spacers to optimize RF homogeneity. All data were collected at ambient temperature.

For the FSLG decoupling,[17, 18] a proton RF power of 102 kHz was used, which corresponds to an effective LG nutation frequency of 125 kHz. Prior to the experiments, the efficiency of the FSLG decoupling was optimized on a preparation of natural abundance adamantane. This was done by observing the J_{CH} couplings in 1D ^{13}C spectra collected with FSLG irradiation during data acquisition, and by fine-tuning of the LG offset frequencies and appropriate timing of delays to yield optimally resolved doublet and triplet line shapes for the CH and CH_2 moieties, respectively. The resultant offset frequencies are about 5% higher than the values calculated from the ^1H nutation frequency. A slight increase of the offset frequency above a LG condition generally results in a more favorable scaling factor, while the additional line broadening as the consequence of a slight deviation from optimal LG irradiation is only very moderate. The ^1H chemical shift scaling factor for the FSLG experiments was determined experimentally on a preparation of [U-^{13}C] tyrosine-HCl, by correlating the scaled proton shifts from an FSLG experiment to the corresponding nonscaled proton shifts obtained with CP wide-line separation correlation spectroscopy[30] at a moderately high field (11.8 T) and fast MAS (25.0 kHz).[21, 31] Following an analogous procedure to that for the ^{13}C assignment,[8, 23] the proton response was initially calibrated by setting the shift of the A55 H^β to $\delta = -0.06$, which is its value in solution at pH 7.3. Since this leads to a systematic shift of $+0.18$ for the other proton resonances, the δ_{solid} values listed in Table 1 have been recalibrated by setting the shift of A55 H^β to $\delta = -0.24$.

All cross-polarization units contained a ramped spin-lock pulse on the carbon nuclei to broaden the CP matching profile at high MAS frequencies (RAMP-CP).[32] Selective heteronuclear polarization transfer was achieved using LGCP.[33–35] A moderate proton RF power corresponding to a ^1H nutation frequency of 48 kHz was applied for the LGCP. Proton decoupling was achieved by use of the two-pulse phase-modulation (TPPM) decoupling scheme during all ^{13}C acquisition periods and during ^{13}C evolution and mixing in the 3D (^1H–^{13}C–^{13}C) correlation experiments.[36] A pulse length of 7.0 μs and a phase-modulation angle of 20 degrees were used for the TPPM decoupling.

The 2D ^1H–^{13}C heteronuclear dipolar correlation spectra were recorded at a MAS frequency of $\omega R/2\pi = 11.5$ kHz with the pulse sequence depicted in Figure 1 A. Following ^1H excitation, the protons are allowed to evolve for a time t_1 under simultanuous FSLG decoupling.[17, 18] The plane of the ^1H nutation is perpendicular to an axis that is inclined at the magic angle with respect to the *z* axis, and the magic-angle pulse at the end of t_1 rotates components of the ^1H signal into the *xy* plane. The LGCP selects and spin-locks the component of the ^1H signal that is parallel to the effective field, while the ^{13}C spins are on-resonance locked in the *xy* plane. In this way, heteronuclear spin-locking is achieved, while simultaneously the ^1H homonuclear dipolar interactions are significantly suppressed. The phase cycling of the pulses is indicated in the figure caption. Additional shifts were applied to the phases $\phi 1$, $\phi 4$, and $\phi 5$ to compensate for the phase jumps during a frequency switch. The phases of the proton preparation pulse, the FSLG sequence, and the magic-angle pulse are varied according to a time-proportional phase incrementation (TPPI) scheme to simulate phase-sensitive detection in t_1.[37]

The 3D (^1H–^{13}C–^{13}C) heteronuclear dipolar correlation spectrum was recorded at a MAS frequency of $\omega R/2\pi = 8.0$ kHz. The 3D dipolar correlation method combines the 2D ^{13}C homonuclear RFDR technique[2, 25] with the 2D ^1H–^{13}C FSLG decoupled spectroscopy of Figure 1 A. The pulse sequence for the 3D spectroscopy is shown in Figure 1 B. The phase of the ^{13}C RAMP-CP spin-lock pulse was varied according to a TPPI scheme, while a TPPI supercycle was applied to the proton pulses. The exchange of polarization through homonuclear ^{13}C dipolar interactions during τ_m was promoted by the use of an integral multiple of XY-8 phase-alternated rotor-synchronized trains of π-pulses as described previously.[2] Low power ^{13}C π pulses of $\approx$23 μs were applied to avoid signal losses due to unwanted CP during the carbon recoupling. A short LGCP contact time of 350 μs was used to minimize ^1H homonuclear coherence exchange during CP, while the RFDR mixing time was kept relatively short (2.0 ms) to avoid exchange of proton modulation through recoupling of the carbon spins.

For the proton assignment in solution at pH 7.3, homonuclear 2D TOCSY, heteronuclear ^{13}C–^1H HSQC, 3D HBHA(CO)NH, and H(CCO)NH-TOCSY spectra were recorded at room temperature (300 K) on a Bruker DMX-400 spectrometer operating at a proton frequency of 400.13 MHz. The assignment process was achieved by the ^1H and ^{15}N chemical shifts published by Blanco et al.[27] Work to compare in detail heteronuclear solid-state and solution shifts of the SH3 domain at different pH values and at different temperatures is in preparation.

Support from the DFG (grant no.: SFB 449) and from the EU (grant no.: BIO4-CT97-2101) is gratefully acknowledged. We wish to thank Rüdiger Winter and Bernd Simon for supply of the ^1H NMR chemical shifts in solution at pH 3.5. Jutta Pauli is supported by the HSPIII.

[1] R. G. Griffin, *Nat. Struct. Biol. NMR Suppl.* **1998**, *7*, 508 – 512.
[2] G. J. Boender, J. Raap, S. Prytulla, H. Oschkinat, H. J. M. de Groot, *Chem. Phys. Lett.* **1995**, *237*, 502 – 508.
[3] B. Q. Sun, P. R. Costa, R. G. Griffin, *J. Magn. Reson. A* **1995**, *112*, 191 – 198.
[4] B. Q. Sun, C. M. Rienstra, P. R. Costa, J. R. Williamson, R. G. Griffin, *J. Am. Chem. Soc.* **1997**, *119*, 8540.
[5] S. K. Straus, T. Bremi, R. R. Ernst, *J. Biomol. NMR* **1998**, *12*, 39 – 50.
[6] B.-J. van Rossum, G. J. Boender, F. M. Mulder, J. Raap, T. S. Balaban, A. Holzwarth, K. Schaffner, S. Prytulla, H. Oschkinat, H. J. M. de Groot, *Spectrochim. Acta A* **1998**, *54*, 1167 – 1176.
[7] A. McDermott, T. Polenova, A. Bockmann, K. W. Zilm, E. K. Paulsen, R. W. Martin, G. T. Montelione, *J. Biomol. NMR* **2000**, *16*, 209 – 219.
[8] J. Pauli, M. Baldus, B. van Rossum, H. de Groot, H. Oschkinat, *ChemBioChem* **2001**, *2*, 272 – 281.
[9] A. Ramamoorthy, L. M. Gierasch, S. J. Opella, *J. Magn. Reson. B* **1996**, *111*, 81 – 84.
[10] F. M. Mulder, W. Heinen, M. van Duin, J. Lugtenburg, H. J. M. de Groot, *J. Am. Chem. Soc.* **1998**, *120*, 12 891 – 12 894.
[11] M. Wilhelm, H. Feng, U. Tracht, H. W. Spiess, *J. Magn. Reson.* **1998**, *134*, 255 – 260.
[12] K. Saalwächter, R. Graf, H. W. Spiess, *J. Magn. Reson.* **1999**, *140*, 471 – 476.
[13] B.-J. van Rossum, C. P. de Groot, V. Ladizhansky, S. Vega, H. J. M. de Groot, *J. Am. Chem. Soc.* **2000**, *122*, 3465 – 3472.
[14] S. P. Brown, I. Schnell, J. D. Brand, K. Müllen, H. W. Spiess, *J. Am. Chem. Soc.* **1999**, *121*, 6712 – 6718.
[15] I. Schnell, S. P. Brown, H. Y. Low, H. Ishida, H. W. Spiess, *J. Am. Chem. Soc.* **1998**, *120*, 11 784 – 11 795.
[16] M. Lee, W. I. Goldburg, *Phys. Rev. A* **1965**, *140*, 1261 – 1271.

[17] A. Bielecki, A. C. Kolbert, M. H. Levitt, *Chem. Phys. Lett.* **1989**, *155*, 341 – 346.
[18] B.-J. van Rossum, H. Förster, H. J. M. de Groot, *J. Magn. Reson*. **1997**, *124*, 516 – 519.
[19] E. Vinogradov, P. K. Madhu, S. Vega, *Chem. Phys. Lett.* **1999**, *314*, 443 – 450.
[20] S. Hafner, H. W. Spiess, *J. Magn. Reson. A* **1996**, *121*, 160 – 166.
[21] B.-J. van Rossum, G. J. Boender, H. J. M. de Groot, *J. Magn. Reson. A* **1996**, *120*, 274 – 277.
[22] S. Ray, E. Vinogradov, G. J. Boender, S. Vega, *J. Magn. Reson.* **1998**, *135*, 418 – 426.
[23] J. Pauli, B. van Rossum, H. Förster, H. J. M. de Groot, H. Oschkinat, *J. Magn. Reson.* **2000**, *143*, 411 – 416.
[24] Z. Gan, *J. Magn. Reson.* **2000**, *143*, 136 – 143.
[25] A. E. Bennett, J. H. Ok, R. G. Griffin, S. Vega, *J. Chem. Phys.* **1992**, *96*, 8624 – 8627.
[26] This assignment is not obvious from the present data. However, current work to assign the amide protons confirmed that the NH signals observed by T32 C^{α} are at the shifts of L33 NH and T32 NH.
[27] F. J. Blanco, A. R. Ortiz, L. Serrano, *J. Biomol. NMR* **1997**, *9*, 347 – 357.
[28] A. Musacchio, M. Noble, R. Pauptit, R. K. Wierenga, M. Saraste, *Nature* **1992**, *359*, 851 – 855.
[29] C. Giessner-Prettre, B. Pullman, *J. Theor. Biol.* **1971**, *31*, 287 – 294.
[30] Data provided by S. Steuernagel (Bruker Analytik GmbH, Karlsruhe, Germany).
[31] K. Schmidt-Rohr, J. Clauss, H. W. Spiess, *Macromolecules* **1992**, *25*, 3273.
[32] G. Metz, X. Wu, S. O. Smith, *J. Magn. Reson. A* **1994**, *110*, 219 – 227.
[33] P. Caravatti, G. Bodenhausen, R. R. Ernst, *Chem. Phys. Lett.* **1982**, *89*, 363 – 367.
[34] C. H. Wu, A. Ramamoorthy, S. J Opella, *J. Magn. Reson. A* **1994**, *109*, 270.
[35] B. van Rossum, S. Prytulla, H. Oschkinat, H. J. M. de Groot in *Magnetic Resonance and Related Phenomena*, *Vol. 5* (Eds.: D. Ziessow, W. Lubitz, F. Lendzian), Technische Universität, Berlin, **1998**, pp. 38 – 39.
[36] E. Bennett, C. M. Rienstra, M. Auger, K. V. Lakshmi, R. G. Griffin, *J. Chem. Phys.* **1995**, *103*, 6951 – 6957.
[37] Redfield, S. D. Kunz, *J. Magn. Reson.* **1975**, *19*, 250.

Received: April 6, 2001 [F 231]